

Lattice collapse and quenching of magnetism in CaFe_2As_2 under pressure: A single crystal neutron and x-ray diffraction investigation

A. I. Goldman^{1,2}, A. Kreyssig^{1,2}, K. Prokeš³, D. K. Pratt^{1,2}, D. N. Argyriou³, J. W. Lynn⁴,
S. Nandi^{1,2}, S. A. J. Kimber³, Y. Chen^{4,5}, Y. B. Lee^{1,2}, G. Samolyuk^{1,2}, J. B. Leão⁴,
S. J. Poulton^{4,5}, S. L. Bud'ko^{1,2}, N. Ni^{1,2}, P. C. Canfield^{1,2}, B. N. Harmon^{1,2} and R. J. McQueeney^{1,2}

¹Ames Laboratory, US DOE, Iowa State University, Ames, IA 50011, USA

²Department of Physics and Astronomy, Iowa State University, Ames, IA 50011, USA

³Helmholtz-Zentrum Berlin für Materialien und Energie, Glienicker Str. 100, 14109 Berlin, Germany

⁴NIST Center for Neutron Research, National Institute of Standards and Technology, Gaithersburg, MD 20899, USA

⁵Department of Materials Science and Engineering, University of Maryland, College Park, MD 20742, USA

(Dated: November 2, 2018)

Single crystal neutron and high-energy x-ray diffraction have identified the phase lines corresponding to transitions between the ambient-pressure tetragonal (T), the antiferromagnetic orthorhombic (O) and the non-magnetic collapsed tetragonal (cT) phases of CaFe_2As_2 . We find no evidence of additional structures for pressures up to 2.5 GPa (at 300 K). Both the T-cT and O-cT transitions exhibit significant hysteresis effects and we demonstrate that coexistence of the O and cT phases can occur if a non-hydrostatic component of pressure is present. Measurements of the magnetic diffraction peaks show no change in the magnetic structure or ordered moment as a function of pressure in the O phase and we find no evidence of magnetic ordering in the cT phase. Band structure calculations show that the transition results in a strong decrease of the iron 3d density of states at the Fermi energy, consistent with a loss of the magnetic moment.

PACS numbers: 61.50.Ks, 61.05.fm, 74.70.Dd

The discovery^{1,2} of pressure-induced superconductivity in CaFe_2As_2 has opened an exciting new avenue for investigations of the relationship between magnetism, superconductivity, and lattice instabilities in the iron arsenide family of superconductors. Features found in the compositional phase diagrams of the iron arsenides,³ such as a superconducting region at low temperature and finite doping concentrations, are mirrored in the pressure-temperature phase diagrams. Superconductivity appears at either a critical doping, or above some critical pressure in the AFe_2As_2 ($\text{A}=\text{Ba}, \text{Sr}, \text{Ca}$) or '122' family of compounds, raising questions regarding the role of both electronic doping and pressure, especially in light of the recent observation of pressure induced superconductivity in the related compound, LaFeAsO .⁴ Does doping simply add charge carriers, or are changes in the chemical pressure, upon doping, important as well? What subtle, or striking, modifications in structure or magnetism occur with doping or pressure, and how are they related to superconductivity?

Similar to other members of the AFe_2As_2 ($\text{A}=\text{Ba}, \text{Sr}$) family,^{5,6,7,8} at ambient pressure CaFe_2As_2 undergoes a transition from a non-magnetically ordered tetragonal (T) phase ($a = 3.879(3)$ Å, $c = 11.740(3)$ Å) to an antiferromagnetic (AF) orthorhombic (O) phase ($a = 5.5312(2)$ Å, $b = 5.4576(2)$ Å, $c = 11.683(1)$ Å) below approximately 170 K.^{9,10} In the O phase, Fe moments order in the so called AF2 structure¹¹ with moments directed along the a -axis of the orthorhombic structure.¹⁰ Neutron powder diffraction measurements¹² of CaFe_2As_2 under hydrostatic pressure found that for $p > 0.35$ GPa (at $T = 50$ K), the antiferromagnetic O phase transforms to a new, non-magnetically ordered, collapsed tetragonal (cT) structure ($a = 3.9792(1)$ Å, $c = 10.6379(6)$ Å) with a dramatic decrease in both the unit cell volume (5%) and the c/a ratio (11%). The transition to the cT phase occurs in close proximity to the pressure at which

superconductivity is first observed.¹ Total energy calculations based on this cT structure concluded that the Fe moment is quenched, consistent with the absence of magnetic neutron diffraction peaks.¹²

Since the report of a cT phase in CaFe_2As_2 under pressure, a significant effort has been devoted to understanding the relationship between the cT structure, features observed in resistivity and susceptibility measurements,^{1,13} and the results of local probe measurements such as μSR .¹⁴ Although the neutron powder diffraction measurements demonstrated the loss of magnetic order in the cT phase, subsequent theoretical work has proposed that the Fe moment in the cT phase is not quenched and orders in an alternative Néel state (the so-called AF1 structure).¹⁵ It has also been suggested, from μSR measurements, that a partial volume fraction of static magnetic order coexists with superconductivity over an intermediate pressure range.¹⁴ Most recently, the existence of a new structural phase above 0.75 GPa in CaFe_2As_2 (Phase III in Ref. 13) has been proposed based on resistivity measurements. It is, therefore, important to clearly identify the chemical and magnetic structures of CaFe_2As_2 , and the phase lines that separate them as a function of temperature and pressure, a task best accomplished by neutron and x-ray diffraction measurements.

In this paper, we report on neutron and x-ray single crystal diffraction studies of the pressure-temperature (p - T) magnetic and structural phase diagram of CaFe_2As_2 . We clearly identify the phase boundaries of the T, O and cT phases in the p - T phase diagram and find significant hysteresis associated with transitions to, and from, the cT phase. We find no evidence of additional structural phases¹³ for pressures up to 2.5 GPa. We also demonstrate that the AF2 ordering is associated only with the O phase, and vanishes upon entering the cT phase in agreement with previous powder diffraction measurements.¹² The apparent coexistence between mag-

netic order and superconductivity under pressure¹⁴ most likely arises from coexistence between the O and cT phases under non-hydrostatic measurement conditions. Furthermore, measurements at reciprocal lattice points associated with one of the three-dimensional realizations of the proposed AF1 structure¹⁵ does not reveal any evidence of magnetic order in the cT phase. Finally, we show from band structure calculations that the collapse of the lattice leads to a strong reduction of the Fe 3d density of states at the Fermi energy, consistent with the loss of magnetism in the cT phase.

I. EXPERIMENTAL DETAILS

The single crystals of CaFe_2As_2 used for the diffraction measurements were grown either using a Sn flux as described previously⁹ or from an FeAs flux. The FeAs powder used for the self-flux growth was synthesized by reacting Fe and As powders after they were mixed and pressed into pellets. The pellets were sealed inside a quartz tube under one-third of an atmosphere of Ar gas, slowly heated to 500° C, held at that temperature for ten hours, and then slowly heated to 900° C and held at 900° C for an additional ten hours. Single crystals of CaFe_2As_2 were grown from this self flux using conventional high-temperature solution growth techniques. Small Ca chunks and the FeAs powder were mixed together in a 1:4 ratio. The mixture was placed into an alumina crucible, together with a second catch crucible containing quartz wool, and sealed in a quartz tube under one-third of an atmosphere of Ar gas. The sealed quartz tube was heated to 1180° C for 2 hours, cooled to 1020° C over 4 hours, and then slowly cooled to 970° C over 27 hours where the FeAs was decanted from the plate like single crystals. The as-grown crystals were annealed at 500° C for 24 hours.

Neutron diffraction data were taken on the BT-7 spectrometer at the NIST Center for Neutron Research and on the E4 diffractometer at the Helmholtz-Zentrum Berlin für Materialien und Energie. High-energy x-ray diffraction data were acquired using station 6-ID-D in the MUCAT Sector at the Advanced Photon Source.

Since much of the description below involves diffraction measurements in both the tetragonal and orthorhombic phases of CaFe_2As_2 , it is useful to describe the indexing system employed in our discussions. For the orthorhombic structure we employ indices $(HKL)_O$ for the reflections based on the relations, $H = h + k$, $K = h - k$ and $L = l$, where $(hkl)_T$ are the corresponding Miller indices for the tetragonal phase. For example, the $(220)_T$ tetragonal peak becomes the orthorhombic $(400)_O$ below the structural transition. The $(hhl)_T$ reciprocal lattice plane in the tetragonal structure becomes the $(HOL)_O$ plane in the orthorhombic phase. The indexing notation for the collapsed tetragonal phase is identical to that for the tetragonal structure. When referring to diffraction peaks, we will use subscripts T, O and cT to denote whether the peaks are indexed in the tetragonal, orthorhombic or collapsed tetragonal phase.

Neutron diffraction measurements on BT-7: Three sets of measurements were performed on the BT-7 diffractometer.

The first data set focused on measurements of phase boundaries separating the T, O and cT phase. These data were taken in double-axis mode, using a wavelength of $\lambda = 2.36 \text{ \AA}$ and two pyrolytic graphite filters to reduce higher harmonic content of the beam. A 10 mg single crystal ($3 \times 3 \times 0.2 \text{ mm}^3$), wrapped in Al-foil was secured to a flat plate within the Al-alloy He-gas pressure cell and cooled using a closed-cycle refrigerator. The sample was oriented so that the $(hhl)_T$ reciprocal lattice plane was coincident with the scattering plane of the diffractometer. The second set of data focused on measurements of the magnetic scattering in the orthorhombic phase. To maximize the intensity of the magnetic scattering relative to the substantial background from the pressure cell, these data were taken on a composite of eight single crystals, attached to a support plate using Fomblin oil, with the diffractometer operated in triple-axis mode using a PG(002) analyzer. The single crystals (combined mass of approximately 60 mg) were co-aligned so that their common $(hhl)_T$ plane was aligned in the scattering plane. The mosaic of the composite sample with respect to the $[hh0]_T$ and $[00l]_T$ directions was approximately 1 deg full-width-at-half-maximum (FWHM). The third data set focused on a survey of magnetic scattering vectors in the $(hol)_{cT}$ diffraction plane of the cT phase associated with the proposed AF1 structure using the same diffractometer conditions as for data set two. For these measurements, a 70 mg single crystal, grown in an FeAs flux, was wrapped in Al-foil and secured to a flat plate within the Al-alloy He-gas pressure cell. The crystal mosaic of this sample was measured to be approximately 1 deg (FWHM).

All of these measurements employed an Al-alloy He-gas pressure cell to ensure hydrostatic pressure conditions. The cell was connected to a pressurizing intensifier through a high pressure capillary that allowed continuous monitoring and adjusting of the pressure. Using this system, the pressure could be varied at fixed temperatures (above the He solidification line), or the temperature could be scanned at nearly constant pressures. A helium reservoir allowed the pressure to remain relatively constant as temperature was changed. The finite size of the reservoir, however, results in some change in pressure over the temperature range measured, on the order of 15% for the highest pressures ($\sim 0.6 \text{ GPa}$).

Neutron diffraction measurements on E4: Additional neutron diffraction data were measured up to a pressure of 1 GPa on the E4 double axis diffractometer with $\lambda = 2.44 \text{ \AA}$ for the $(hhl)_T$ orientation of a 10 mg Sn-flux grown single crystal. Here we employed a Be-Cu clamp-type pressure cell and a 1:1 mixture of Fluorinert 77 and 70, for the pressure medium. The pressure was set *ex-situ* at room temperature and the cell was inserted into a standard He cryostat. The initial pressure was measured using a manganin pressure sensor and then monitored *in-situ* (since pressure decreases with decreasing temperature) by tracking the lattice constants of NaCl crystals placed above the sample.

High-energy x-ray diffraction measurements: In order to move beyond the limits of the He-gas and clamped pressure cells we used a Merrill-Bassett diamond anvil pressure cell with an ethanol/methanol mixture as the pressure medium. This cell allowed us to collect diffraction data at 300K up

to 2.5 GPa. Here we employed 100 keV x-rays to ensure full penetration of single crystal (Sn-flux grown) samples in the cell and recorded diffraction data over layers of reciprocal space using a 2D detector. At all pressures investigated the medium remained fluid.

II. RESULTS

A. Determination of the pressure-temperature phase diagram

We first describe how the temperature/pressure phase lines for CaFe_2As_2 , shown in Fig. 1(a), were derived from our neutron and high-energy x-ray diffraction measurements. The T-O phase boundary was determined by monitoring the $(220)_T$ or $(112)_T$ diffraction peaks upon heating (solid circles) or cooling (open circles) at specified pressures. At the T-O transition, the orthorhombic distortion and associated twinning splits both the $(220)_T$ and $(112)_T$ peaks, providing a clear signature of the transition. As indicated in Fig. 1(a), there is little hysteresis in the T-O transition (~ 2 -3 K), consistent with our previous measurements at ambient pressure.^{1,9,10}

In a similar fashion, the T-cT phase boundary in Fig. 1(a) was mapped by monitoring the intensity of the $(004)_{cT}$ peak while heating the sample from low temperature (solid squares), or the intensity of the $(004)_T$ diffraction peak while cooling the sample from higher temperature (open squares). The sizeable difference ($\sim 9\%$) in the c -lattice constants for these two structures is evident from the scattering angles for the two peaks in Figs. 1(b) and (c). Figure 1(d) shows that, at a nominal pressure of 0.47 GPa, the cT phase transforms sharply to the T phase at 141 K (on heating) with no coexistence beyond the 1 K wide transition region. On decreasing temperature, the transition from the T to the cT phase is also very sharp but occurs at 112 K, nearly 30 K below the transition on heating, demonstrating the strong hysteresis (similar in magnitude noted in Refs. 1 and 13) in the T-cT transition. We also point out that the strong volume changes associated with the T-cT transition irreversibly increases the sample mosaic. Indeed, the difference between the measured peak intensities for the (004) diffraction peaks in Fig. 1(d) arises from the doubling of the sample mosaic during this transition. We note, however, that all transitions in temperature and pressure were reproducible, even after several pressure/temperature cycles.

The phase boundary between the O and the cT phases was determined by increasing/decreasing pressure at a fixed temperature while monitoring the $(004)_O$ diffraction peak (increasing pressure, solid triangles) and the $(004)_{cT}$ peak (decreasing pressure, open triangles). For example, at 92 K, on increasing pressure, a sharp transition from the O to cT phase, with a width smaller than our step size of 0.025 GPa, was found between 0.375 and 0.400 GPa (Fig. 1(e)). Upon decreasing pressure at 92 K, however, the transition to the O phase occurred at 0.225 GPa (Fig. 1(f)), demonstrating a striking pressure hysteresis in the O-cT transition as well. Nevertheless, the transitions themselves were sharp with no phase coexistence in evidence. We note that above 0.4 GPa, the cT phase persists down to the lowest temperature (4 K) and high-

est pressure (0.6 GPa) attained for the BT-7 measurements.

Based upon resistivity measurements performed in a clamp-type Be-Cu cell using a silicon fluid as a pressure medium, Lee *et al.*¹³ have proposed that there is a transition at approximately 0.75 GPa from the cT phase to another structure of unknown symmetry (Phase III in Ref. 13). In order to move beyond the limits of the He-gas pressure cell to investigate the possibility of additional phases at higher pressure, x-ray diffraction measurements were performed using a diamond-anvil pressure cell at 300 K on the 6ID-D station in the MU-CAT Sector at the Advanced Photon Source. Diffraction data over a wide range of reciprocal space in both the $(hhl)_T$ and $(hol)_T$ planes were collected using a two-dimensional area detector. As described in earlier work,¹⁶ entire reciprocal lattice planes can be imaged to identify any new reflections that signal the presence of additional structural phases. The T-cT transition at 300 K is evidenced by the strong change in lattice constants observed at 1.6 GPa, as shown in the inset of Fig. 1(a). No additional diffraction peaks were found above this transition, confirming the presence of only the cT phase for pressures up to 2.5 GPa.

One of the most striking features of Fig. 1(a) is the large hysteresis regime represented by the shading. Within this area, the structure and physical properties measured at a particular pressure and temperature depend strongly upon the path taken to that point. Taken together, this large range of hysteresis and the strongly anisotropic response of the structure at the cT phase boundaries (see discussion in Section IIC) can easily lead to discrepancies in reports of magnetic order, electronic properties and superconductivity in CaFe_2As_2 under pressure.

B. The magnetic structure of CaFe_2As_2 under pressure

One of the most interesting results of the original report of a cT phase from neutron powder diffraction measurements,¹² was the disappearance of Fe magnetic ordering. The antiferromagnetic AF2 ordering in the orthorhombic phase of CaFe_2As_2 is shown in Fig. 2(a). Magnetic diffraction peaks are found at positions $(HOL)_O$ with H and L odd, such as $(101)_O$ and $(103)_O$. During the course of our measurements of the single crystal on BT-7 the magnetic peaks were also monitored. The $(101)_O$ and $(103)_O$ magnetic peaks were observed (see, for example, Fig. 1(h)) at selected pressures and temperatures within the O phase, but no AF2 magnetic peaks were found at the corresponding $(\frac{1}{2}\frac{1}{2}1)$ or $(\frac{1}{2}\frac{1}{2}3)$ positions (see Figs. 1(g) and (i)) in either the T or cT phases, consistent with previous results.¹²

In order to more closely track the evolution of the magnetic structure with pressure, a composite sample of eight single crystals, as described in the Section I, was mounted in the He-gas pressure cell and cooled through the T-O transition at ambient pressure. At $T = 75$ K, pressure was increased in 0.05 GPa steps, through the O-cT transition, up to a maximum pressure of 0.45 GPa. The temperature was then lowered to 50 K and pressure was released in 0.05 GPa steps to ambient pressure. At each pressure step, the $(004)_O$ and $(004)_{cT}$ nu-

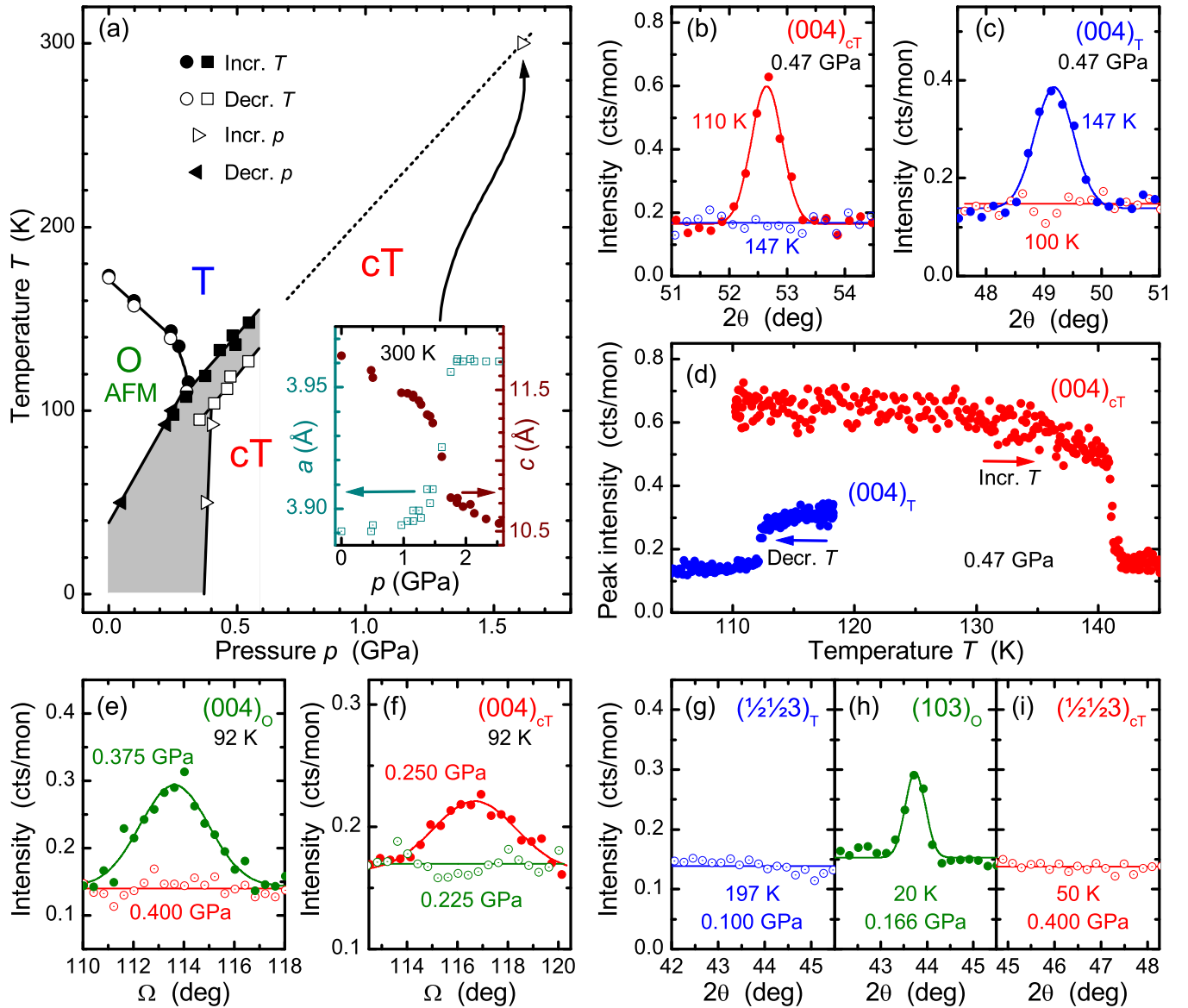


FIG. 1: (color online) (a) Pressure-temperature phase diagram of CaFe_2As_2 under hydrostatic pressure determined from neutron and high-energy x-ray diffraction measurements. Filled and open circles (squares) denote phase boundaries determined upon heating and cooling at a set pressure for the O-T (cT-T) phase transition, respectively. Filled and open triangles denote phase boundaries determined upon increasing and decreasing pressure at a fixed temperature, respectively. The shaded area denotes the hysteretic region. The inset of Fig. 1(a) shows the change in lattice constants at the T-cT transition at 300 K as measured by high-energy x-ray diffraction. In Figs. 1(b)-(i), the color codes denote measurements of the T phase (blue), O phase (green) or cT phase (red) diffraction peak positions. In Figs. 1(b)-(c), the color codes denote measurements of the $(004)_{\text{cT}}$ peak at 0.47 GPa on increasing temperature. Here Ω denotes the sample angle while 2θ is the scattering angle. (c) Ω - 2θ scans of the $(004)_{\text{T}}$ peak at 0.47 GPa on decreasing temperature. (d) Temperature dependence of the peak intensities of the $(004)_{\text{T}}$ as temperature is decreased through the T-cT transition at $p=0.47$ GPa, and the $(004)_{\text{cT}}$ as temperature is increased through the T-cT transition at $p=0.47$ GPa. (e) Ω scans through the $(004)_{\text{O}}$ peak at 92 K as the pressure is increased from 0.375 to 0.400 GPa. (f) Ω scans through the $(004)_{\text{cT}}$ peak at 92 K as the pressure is decreased from 0.250 to 0.225 GPa. (g) Ω - 2θ scans through the expected position of the $(\frac{1}{2}\frac{1}{2}3)_{\text{T}}$ magnetic peak in the tetragonal phase. (h) Ω - 2θ scans through the observed position of the $(103)_{\text{O}}$ magnetic peak in the orthorhombic phase. (i) Ω - 2θ scans through the expected position of the $(\frac{1}{2}\frac{1}{2}3)_{\text{cT}}$ magnetic peak in the collapsed tetragonal phase.

clear peaks were measured along with the $(101)_{\text{O}}$ and $(103)_{\text{O}}$ magnetic peaks.

Fig. 3 plots the volume fraction of the O and cT phases as a function of pressure at these two temperatures, deter-

mined from the integrated intensities of the $(004)_{\text{O}}$ and $(004)_{\text{cT}}$ peaks. The integrated intensity of the $(103)_{\text{O}}$ magnetic peak is also plotted at each pressure value. Upon increasing pressure at 75 K, the magnetic peak intensity remains constant

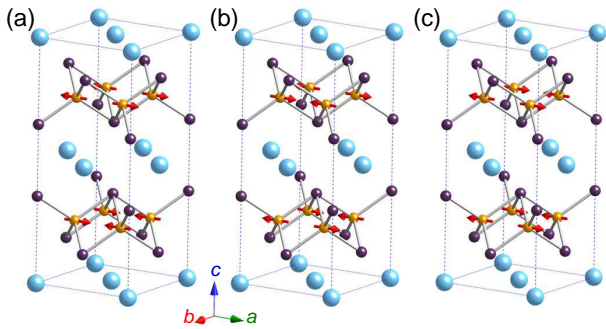


FIG. 2: (color online) Magnetic structures for CaFe_2As_2 shown in the orthorhombic unit cell to facilitate comparison. (a) The AF2 magnetic structure realized at ambient pressure below 170 K.¹⁰ (b) Representation of the AF1 G-type antiferromagnetic structure with antiferromagnetic ordering along the c -axis. (c) Representation of the AF1 C-type antiferromagnetic structure with ferromagnetic ordering along the c -axis.

until the O-cT phase boundary is reached. At 0.40 GPa we observe coexistence between the O and cT phases and a decrease in the magnetic intensity consistent with the decrease in O phase volume fraction. For pressures greater than 0.45 GPa, the sample has completely transformed to the cT phase and there is no evidence of static antiferromagnetic order associated with the AF2 structure at either the $(103)_\text{O}$ or $(\frac{1}{2}\frac{1}{2}3)_\text{cT}$ reciprocal lattice positions. As pressure is decreased at 50 K, only the cT phase is present until the cT-O transition boundary at 0.075 GPa, consistent with the results shown in Fig. 1(a). Upon the appearance of the O phase, the AF2 structure is once again recovered.

One interesting difference between the data in Fig. 3 and Fig. 1 is the finite range of coexistence between the O and cT phases. In particular, we see that for the composite sample, the cT phase is evident down to ambient pressure whereas for the single crystal sample, the transition between the cT and O phases was sharp, exhibiting little in the way of phase coexistence. We attribute this to the fact that the composite sample was set on a sample holder using Fomblin oil, which solidifies well above the temperatures of these measurements. As described below, dramatic changes in the unit cell dimensions, as the sample transforms into (or out of) the cT phase, can introduce significant strain for constrained samples that "smears" the transition. Nevertheless, these data show that: (1) the AF2 magnetic structure is associated with the O phase and is absent in the cT phase and; (2) The magnetic moment associated with the AF2 structure is independent of pressure up to the O-cT transition.

Although the neutron powder diffraction measurements demonstrated the loss of magnetic order in the cT phase, subsequent first-principles calculations¹⁵ have claimed that the cT phase is magnetic and Fe moments order in a AF1 Néel state (all nearest neighbor interactions are AF) with a moment of $1.3 \mu_B$. There are two three-dimensional realizations of the AF1 structure, illustrated in Fig. 2, with either an antiferromagnetic (Fig. 2(b)) or ferromagnetic (Fig. 2(c)) alignment

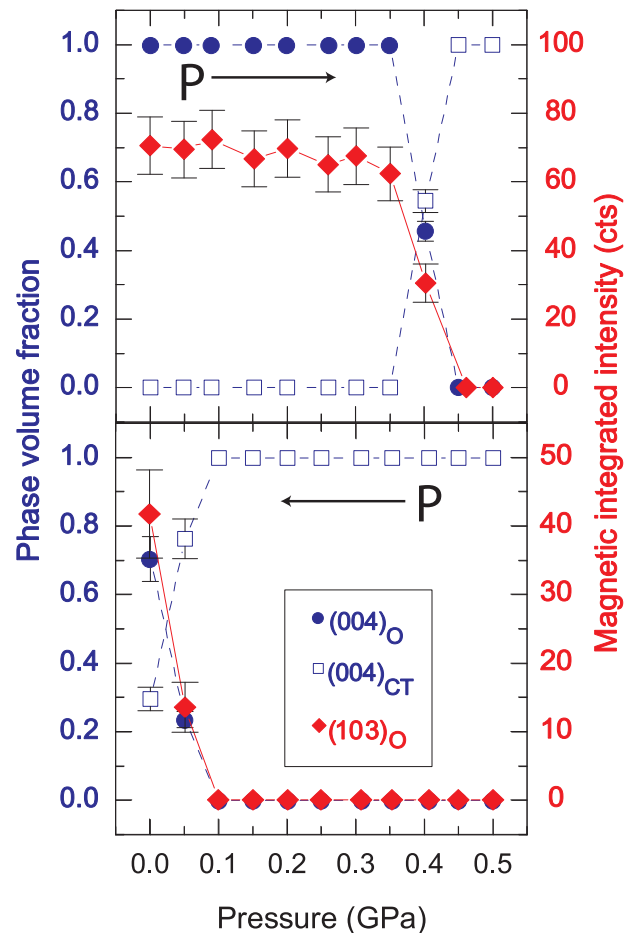


FIG. 3: (color online) Phase fractions of the O and cT phases as a function of pressure upon increasing pressure (top panel) at 75 K and decreasing pressure (bottom panel) at 50 K. The integrated intensity of the magnetic $(103)_\text{O}$ reflection remains constant in the O phase.

of adjacent Fe planes along the c -axis. For both cases, the magnetic unit cell is the same as the chemical unit cell. For the structure in Fig. 2(b), magnetic reflections will be found at positions $(h0l)_\text{cT}$ with h and l odd. Unfortunately, these positions also correspond to allowed nuclear reflections and, unless the moment is large, the magnetic contribution to the scattering is difficult to measure using unpolarized neutrons. For the structure illustrated in Fig. 2(c), magnetic reflections will be found at positions $(h0l)_\text{cT}$ with h odd and l even. These positions are forbidden for nuclear scattering from the $I4/mmm$ tetragonal structure and were investigated using the 70 mg FeAs-flux grown sample. Measurements were done at ambient pressure and $T = 167$ K (in the O phase for reference) and at $p = 0.62$ GPa and $T = 50$ K (in the cT phase). We found no evidence of AF1 magnetic order at the $(100)_\text{cT}$ and $(102)_\text{cT}$ positions, consistent with our previous neutron diffraction measurements.¹²

C. Coexistence of phases in CaFe_2As_2 under pressure

While our single crystal data (Section IIA) clearly shows the presence of single phase fields in the p-T phase diagram, we do find circumstances in which extended ranges of coexistence between the cT and O or T phases occur. We believe that this observation is key to understanding recent μSR measurements that suggest that a partial volume fraction of static magnetic order coexists with superconductivity over an intermediate pressure range.¹⁴ For example, in Fig. 4 we show the evolution of the $(002)_T$ diffraction peak as a function of temperature at 0.83 GPa (set at room temperature) measured on the E4 diffractometer using a Be-Cu clamp-type pressure cell and a 1:1 mixture of Fluorinert 77 and 70, for the pressure medium. On decreasing the temperature below approximately 120 K ($P = 0.66(5)$ GPa), we find evidence of an extended coexistence regime between the T and O phases. As temperature is further decreased below approximately 100 K ($P = 0.60(5)$ GPa), Fig. 4 shows coexistence between the O and cT structures that persists down to the base temperature of 2 K.

The coexistence of the antiferromagnetic O and the non-magnetic cT phase under conditions similar to those for the μSR measurements,¹⁴ provides a compelling explanation for the observed coexistence between static magnetic order, with a volume fraction that decreases with increasing pressure, and a non-magnetic volume fraction, that increases with increasing pressure. We attribute this behavior to the freezing of the pressure mediating liquid above 150K (Daphne oil 7373¹⁷ in ref 14 and Fluorinert here). This freezing, coupled with the anisotropy in the change across the T-cT transition, can lead to significant pressure gradients through the sample(s), a problem that is not encountered in our He gas cell apparatus for the temperature and pressure ranges investigated here. As noted in Section IIB, bonding the sample to a support can result in similar strains and inhomogeneities, smearing the transitions to and from the cT phase and extending the coexistence regime between phases.

III. DISCUSSION

Although it appears, so far, that the related compounds, BaFe_2As_2 and SrFe_2As_2 do not manifest a cT phase at elevated pressures,¹⁸ the transition to a cT phase in CaFe_2As_2 with applied pressure is not unique among systems that crystallize in the ThCr_2Si_2 structure. Other examples of this phenomenon are found among the phosphide compounds including SrRh_2P_2 and EuRh_2P_2 ,¹⁹ as well as SrNi_2P_2 , EuCo_2P_2 ²⁰ and EuFe_2P_2 .²¹ For the Eu-compounds, the cT phase is accompanied by a valence transition from Eu^{2+} to the non-magnetic Eu^{3+} and, for EuCo_2P_2 , a change from local moment $\text{Eu}(4f)$ to itinerant $\text{Co}(3d)$ magnetism associated with a strong modification of the 3d bands in the cT phase.²² In all of these phosphide compounds, the striking decrease in the c/a ratios in the cT phase has been described in terms of "bonding" transitions involving the formation of a P-P single bond between ions in neighboring planes along the c-axis, and has been discussed in some detail, by Hoffmann

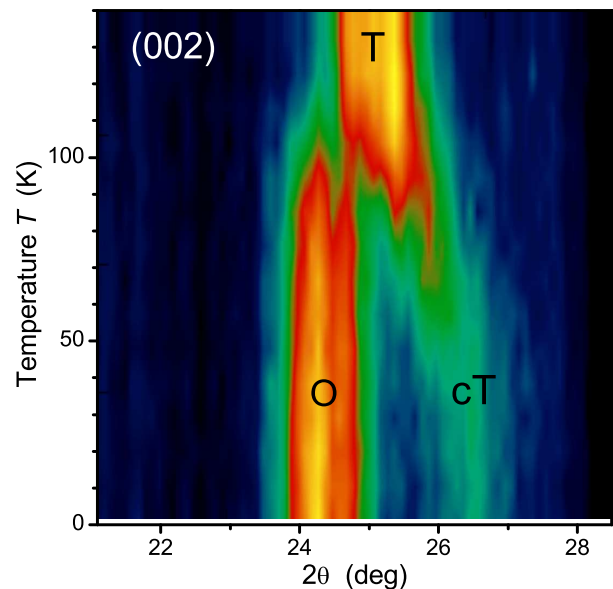


FIG. 4: (color online) Measurement of the (002) nuclear reflection from CaFe_2As_2 with an area detector on the E4 diffractometer using a Be-Cu clamp-type cell. For an initial pressure of 0.83 GPa, at room temperature, the T phase transforms to a mixture of the cT and O phase below approximately 100 K.

and Zheng.²³

Following this work on the small A-site cation limit for the isostructural phosphide compounds,²³ we suggest that there is a transition in the bonding character of As-ions and the promotion of As-As bonds across the Fe_2As_2 layers under pressure. This was also suggested in recent theoretical work by Yildirim.¹⁵ In the ambient pressure tetragonal phase, the As-As distance between neighboring Fe_2As_2 layers is approximately 3.15 Å, much larger than the As-As single bond distance of 2.52 Å in elemental As. In the cT phase, the As-As distance decreases to approximately 2.82 Å, still larger, but much closer to the range of a As-As single bond. The enhancement of the As-As bonding under pressure can have dramatic effects on band structure and magnetism.²³ In the case of the collapsed phase of EuCo_2P_2 , for example, an increase in the Co 3d band-filling results in an enhancement of the density of states at the Fermi energy and the formation of a Co magnetic moment.²¹ It has also been pointed out that even small changes in the arsenic position (z_{As}) strongly affects the occupation of the Fe $3d_{x^2-y^2}$ orbitals and, therefore, the magnetic behavior.²⁴

To further investigate the impact of the cT transition on the electronic density of states (DOS) and generalized susceptibility, $\chi(\mathbf{q})$, of CaFe_2As_2 , we have performed band structure calculations for both the T and cT phases. These calculations were performed using the full potential LAPW method, with $R_{MT} * K_{\text{max}} = 8$, $R_{MT} = 2.2, 2.0, 2.0$ atomic units for Ca, Fe and As respectively. The number of k-points in the irreducible Brillouin zone are 550 for the self consistent charge, 828 for the DOS calculation, and 34501 for the $\chi(\mathbf{q})$ calcula-

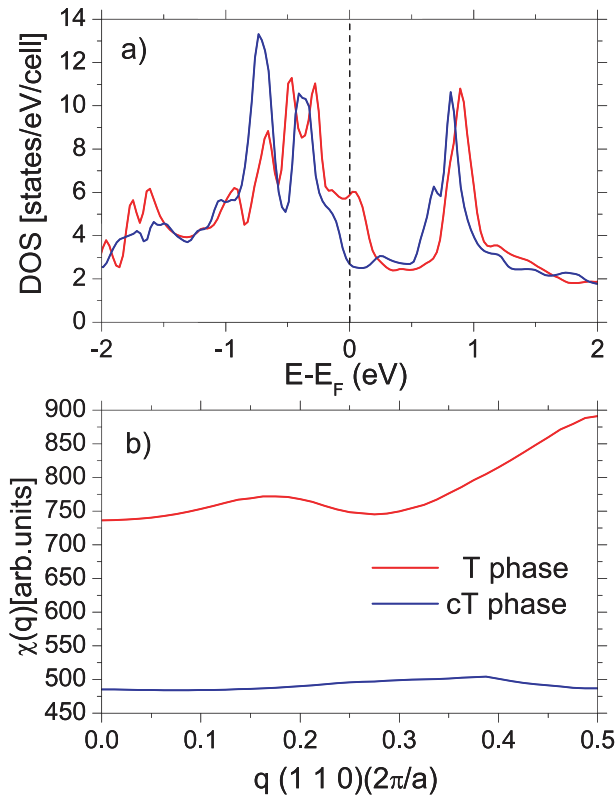


FIG. 5: (color online) (a) Calculated DOS near the Fermi energy for the T (red line) and cT (blue line) phases of CaFe_2As_2 (b) The generalized susceptibility $\chi(q)$ for the T (red line) and cT (blue line) phases of CaFe_2As_2

tion. For the local density functional, the Perdew-Wang 1992 functional²⁵ was employed. The convergence criterion for the total energy was 0.01 mRyd/cell. The structural parameters for the T and cT phases were obtained from experiment.¹² The density of states, obtained with the tetrahedron method, has been broadened with a Gaussian of width 3 mRyd.

Fig. 5(a) shows the calculated density of states (DOS) within 2 eV of the Fermi energy for both non-magnetic tetragonal phases. The Fe states overwhelmingly (> 95 percent) contribute in this region, with significant As hybridization (bonding) occurring at lower energies and Ca contributions appearing at higher energies. The most significant change in the collapsed phase is the dramatic lowering of the DOS at the Fermi energy associated, primarily, with a shift to lower energies of the Fe $3d_{x^2-y^2}$ and Fe $3d_{xz+yz}$ orbitals. This is also demonstrated in the corresponding $\chi(q)$ calculations shown in Fig. 5(b) for the two phases.

The intraband contribution to $\chi(q=0)$ is exactly the density of states at E_F , with a large value favoring ferromagnetic ordering (Stoner criteria). We note that the DOS at E_F of 2.8 states/eV-Fe is comparable to that for pure Fe (3.0 states/eV-Fe). The considerably larger peak in $\chi(q)$ at the zone boundary for the T phase, however, is an indication that the magnetic instability is antiferromagnetic, with ordering observed upon a small orthorhombic distortion.¹⁰ The small DOS at E_F for the

cT phase shown in Fig. 5(a) is not sufficient to induce magnetic ordering, and the essentially featureless $\chi(q)$ (note the offset) in Fig. 5(b) and along other high symmetry directions (not shown) for the cT phase indicates that magnetic ordering is unlikely at any q-vector.

These calculations clearly support the notion of a depressed Fe 3d density of states at E_F , which is consistent with previous work^{15,24,26} as well as the suppression of magnetism in the cT phase. The suppression of the DOS realized in these calculations is, however, surprising in light of the strong reduction in the resistivity of CaFe_2As_2 found upon transformations into the cT phase.^{1,2} This suggests that scattering effects are greatly reduced in the cT phase in comparison to the T phase, and calls for further investigation of the spin-fluctuation spectrum of the T phase in particular.

IV. SUMMARY AND CONCLUSIONS

To summarize our results, we have identified the phase lines corresponding to transitions between the ambient-pressure tetragonal, the antiferromagnetic orthorhombic, and the non-magnetic collapsed tetragonal phases of CaFe_2As_2 . No additional structures for pressures up to 2.5 GPa (at 300 K) were observed, in contradiction to the proposal of Ref 13. For at least one of the two possible AFI structures, we find no evidence of magnetic ordering in the cT phase as proposed in Ref. 15.

Whereas the low-pressure T-O transition presents only slight hysteresis (~ 2 K), both the T-cT and O-cT transitions exhibit very significant hysteresis effects. The large temperature/pressure range of hysteresis, together with the strongly anisotropic changes in the CaFe_2As_2 lattice at the cT transition must be considered in the interpretation of resistivity and susceptibility measurements in CaFe_2As_2 , particularly for measurements where non-hydrostatic pressure effects are possible. We have demonstrated that the μSR measurements in Ref 14 are consistent with our neutron powder and single-crystal studies; the coexistence of non-magnetic and magnetically ordered fractions results from coexistence between the O and cT phases in the presence of a non-hydrostatic pressure component. We also note that pressure-induced superconductivity in CaFe_2As_2 has been observed close to the O-cT transition, and within the hysteretic region associated with that transition and, therefore, should be studied carefully under hydrostatic conditions.

The loss of magnetism in the cT phase is largely due to changes in the band structure that depletes Fe 3d DOS at E_F , a behavior that is analogous to other 122 type compounds^{19,20,21,23} and qualitatively consistent with previous theoretical calculations.^{15,24,26}

The authors wish to acknowledge very useful discussions with Joerg Schmalian, the assistance of J.Q. Yan with sample preparation, and the assistance of Yejun Feng and Doug Robinson with the high energy x-ray measurements. The work at the Ames Laboratory and at the MUCAT sector was supported by the U.S. DOE under Contract No. DE-AC02-07CH11358. The use of the Advanced Photon Source

was supported by U.S. DOE under Contract No. DE-AC02-06CH113.

-
- ¹ M. S. Torikachvili, S. L. Bud'ko, N. Ni, and P. C. Canfield, *Phys. Rev. Lett.* **101**, 057006 (2008).
- ² T. Park, E. Park, H. Lee, T. Klimczuk, E. D. Bauer, F. Ronning, and J. D. Thompson, *J. Phys.: Condens. Matter* **20**, 322204 (2008).
- ³ M. R. Norman, *Physics* **1**, 21 (2008), and references therein.
- ⁴ H. Okada, K. Igawa, H. Takahashi, Y. Kamihara, M. Hirano, H. Hosono, K. Matsubayashi, and Y. Uwatoko, *J. Phys. Soc. Jpn.* **77**, 113712 (2008).
- ⁵ Q. Huang, Y. Qiu, W. Bao, M. A. Green, J. W. Lynn, Y. C. Gasparovic, T. Wu, G. Wu, and X. H. Chen, arXiv:0806.2776 (2008), unpublished.
- ⁶ A. Jesche, N. Caroca-Canales, H. Rosner, H. Borrmann, A. Ormeci, D. Kasinathan, K. Kaneko, H. H. Klauss, H. Luetkens, R. Khasanov, et al., arXiv:0807.0632 (2008), unpublished.
- ⁷ J. Zhao, W. Ratcliff, II, J. W. Lynn, G. F. Chen, J. L. Luo, N. L. Wang, J. Hu, and P. Dai, *Phys. Rev. B* **78**, 140504(R) (2008).
- ⁸ Y. Su, P. Link, A. Schneidewind, T. Wolf, Y. Xiao, R. Mittal, M. Rotter, D. Johrendt, T. Brueckel, and M. Loewenhaupt, arXiv:0807.1743 (2008), unpublished.
- ⁹ N. Ni, S. Nandi, A. Kreyssig, A. I. Goldman, E. D. Mun, S. L. Bud'ko, and P. C. Canfield, *Phys. Rev. B* **78**, 014523 (2008).
- ¹⁰ A. I. Goldman, D. N. Argyriou, B. Ouladdiaf, T. Chatterji, A. Kreyssig, S. Nandi, N. Ni, S. L. Bud'ko, P. C. Canfield, and R. J. McQueeney, *Phys. Rev. B* **78**, 100506(R) (2008).
- ¹¹ T. Yildirim, *Phys. Rev. Lett.* **101**, 057010 (2008).
- ¹² A. Kreyssig, M. A. Green, Y. Lee, G. D. Samolyuk, P. Zajdel, J. W. Lynn, S. L. Bud'ko, M. S. Torikachvili, N. Ni, S. Nandi, et al., arXiv:0807.3032 (2008), unpublished.
- ¹³ H. Lee, E. Park, T. Park, F. Ronning, E. D. Bauer, and J. D. Thompson, arXiv:0809.3550 (2008), unpublished.
- ¹⁴ T. Goko, A. A. Aczel, E. Baggio-Saitovitch, S. L. Bud'ko, P. Canfield, J. P. Carlo, G. F. Chen, P. Dai, A. C. Hamann, W. Z. Hu, et al., arXiv:0808.1425 (2008), unpublished.
- ¹⁵ T. Yildirim, arXiv:0807.3936 (2008), unpublished.
- ¹⁶ A. Kreyssig, S. Chang, Y. Janssen, J. W. Kim, S. Nandi, J. Q. Yan, L. Tan, R. J. McQueeney, P. C. Canfield, and A. I. Goldman, *Phys. Rev. B* **76**, 054421 (2007).
- ¹⁷ K. Murata, H. Yoshino, H. O. Yadav, Y. Honda, and N. Shirakawa, *Rev. Sci. Instrum.* **68**, 2490 (1997).
- ¹⁸ S. A. J. Kimber, A. Kreyssig, F. Yokaichiya, D. N. Argyriou, J. Q. Yan, T. Hansen, T. Chatterji, R. J. McQueeney, P. C. Canfield, and A. I. Goldman (2008), unpublished.
- ¹⁹ C. Huhnt, G. Michels, M. Roepke, W. Schlabitz, A. Wurth, D. Johrendt, and A. Mewis, *Physica B* **240**, 26 (1997).
- ²⁰ C. Huhnt, W. Schlabitz, A. Wurth, A. Mewis, and M. Reehuis, *Phys. Rev. B* **56**, 13796 (1997).
- ²¹ B. Ni, M. M. Abd-Elmeguid, H. Micklitz, J. P. Sanchez, P. Vulliet, and D. Johrendt, *Phys. Rev. B* **63**, 100102(R) (2001).
- ²² M. Chefki, M. M. Abd-Elmeguid, H. Micklitz, C. Huhnt, W. Schlabitz, M. Reehuis, and W. Jeitschko, *Phys. Rev. Lett.* **80**, 802 (1998).
- ²³ R. Hoffmann and C. Zheng, *J. Phys. Chem.* **89**, 4175 (1985).
- ²⁴ C. Krellner, N. Caroca-Canales, A. Jesche, H. Rosner, A. Ormeci, and C. Geibel, *Phys. Rev. B* **78**, 100504(R) (2008).
- ²⁵ J. P. Perdew and Y. Wang, *Phys. Rev. B* **45**, 13244 (1992).
- ²⁶ G. D. Samolyuk and V. P. Antropov, arXiv:0810.1445 (2008), unpublished.